Inorganic Chemistry

Article

pubs.acs.org/IC

Four Dibutylamino Substituents Are Better Than Eight in Modulating the Electronic Structure and Third-Order Nonlinear-Optical Properties of Phthalocyanines

Yuxiang Chen, Wei Cao, Chiming Wang, Dongdong Qi,* Kang Wang, and Jianzhuang Jiang*

Beijing Key Laboratory for Science and Application of Functional Molecular and Crystalline Materials, Department of Chemistry, University of Science and Technology Beijing, Beijing 100083, China

Supporting Information

ABSTRACT: 2(3),9(10),16(17),23(24)-Tetrakis(dibutylamino)-phthalocyanine compounds M{Pc[N(C_4H_9)$_2$]$_4$} (**1**−**5**; M = 2H, Mg, Ni, Cu, Zn) were prepared and characterized by a range of spectroscopic methods in addition to elemental analysis. Electrochemical and electronic absorption spectroscopic studies revealed the more effective conjugation of the nitrogen lone pair of electrons in the dibutylamino side chains with the central phthalocyanine π system in M{Pc[N(C_4H_9)$_2$]$_4$} than in M{Pc[N-(C_4H_9)$_2$]$_8$}, which, in turn, results in superior third-order nonlinear-optical (NLO) properties of H_2{Pc[N(C_4H_9)$_2$]$_4$} (**1**) over H_2{Pc[N(C_4H_9)$_2$]$_8$}, as revealed by the obviously larger effective imaginary third-order molecular hyperpolarizability (Im{$\chi^{(3)}$}) of 6.5×10^{-11} esu for the former species than for the latter one with a value of 3.4×10^{-11} esu. This is well rationalized on the basis of both structural and theoretical calculation results. The present result seems to represent the first effort toward directly connecting the peripheral functional substituents, electronic structures, and NLO functionality together for phthalocyanine molecular materials, which will be helpful for the development of functional phthalocyanine materials via molecular design and synthesis even through only tuning of the peripheral functional groups.

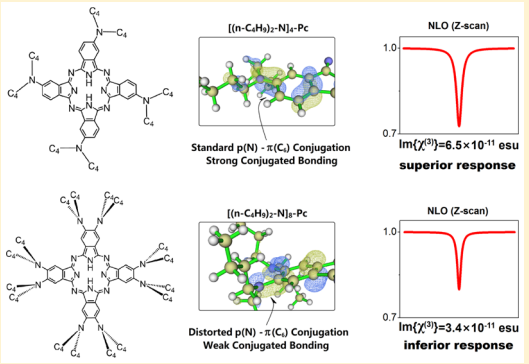

INTRODUCTION

Phthalocyanines have been an important class of dyes and pigments with extensive applications in paint, printing, and textile industries since their serendipitous discovery at the beginning of the past century.[1] More recently, their unique spectroscopic and electrochemical properties in combination with extraordinary chemical and thermal stabilities endow these tetrapyrrole compounds great application potentials as advanced functional materials in the fields of medicine,[2] optical storage,[3] photocatalysis,[4] and molecular-based nanoelectronic devices.[5] For the purpose of enhancing their application-related functionalities, a wide range of different kinds of substituents including the electron-withdrawing nitro, fluoro, chloro, bromo, and iodo groups and the electron-donating alkyl, alkoxyl, ether, and alkylthio groups have been incorporated onto their peripheral and/or nonperipheral positions to modulate their electronic structure and electrochemical and spectroscopic properties.[6] However, amino- and/or alkylamino-substituted phthalocyanines have been relatively less studied despite their significant role in tuning the electronic structure and, in turn, the electrochemical and spectroscopic properties of phthalocyanines expected from their strong electron-donating nature, with corresponding examples limited to tetraaminophthylocyanines,[7] 2,3,9,10,16,17,23,24-octaaminophthalocyaninatonickel,[8] tetrakis[4-chloro-5-(dimethylamino)phthalocyaninato]zinc,[9] tetrakis[4-fluoro-5-(dimethylamino)phthalocyaninato]zinc,[9] octakis[4,5-bis(dimethylamino)-3,6-difluorophthalocyaninato]-zinc,[9] and tetrakis[4-chloro-5-(di-*n*-hexylamino)]-phthalocyanines,[10] to the best of our knowledge. For the purpose of affording new members in this series toward developing novel and improved functionalities, dibutylamino groups have been introduced onto the phthalocyanine periphery very recently.[11] Cyclic tetramerization of 4,5-bis(dibutylamino)phthalonitrile led to the successful isolation of 2,3,9,10,16,17,23,24-octakis(dibutylamino)phthalocyanines. This, however, is not exactly true for the case of 2(3),9(10),16(17),23(24)-tetrakis(dibutylamino)-phthalocyanine counterparts with 4-(dibutylamino)-phthalonitrile instead of 4,5- bis(dibutylamino)phthalonitrile as the precursor because satisfactory ^{1}H NMR spectra could not be obtained for this series of compounds despite their right mass spectroscopic (MS) results. Fortunately, the nature of the ease of tetrakis(dibutylamino)phthalocyanine compounds toward oxidation in comparison with their octakis-(dibutylamino)phthalocyanine counterparts was finally recognized because of their raised highest occupied molecular orbital (HOMO) energy level associated with the more effective conjugation between the dibutylamino nitrogen atoms and phthalocyanine π system, resulting in the successful isolation

Received: January 14, 2016

DOI: 10.1021/acs.inorgchem.6b00100
Inorg. Chem. XXXX, XXX, XXX−XXX

Scheme 1. Synthesis and Schematic Molecular Structures of 2(3),9(10),16(17),23(24)-Tetrakis(dibutylamino)phthalocyanine Compounds M{Pc[N(C_4H_9)$_2$]$_4$} (1−5; M = 2H, Mg, Ni, Cu, Zn) with Four Regioisomers[a]

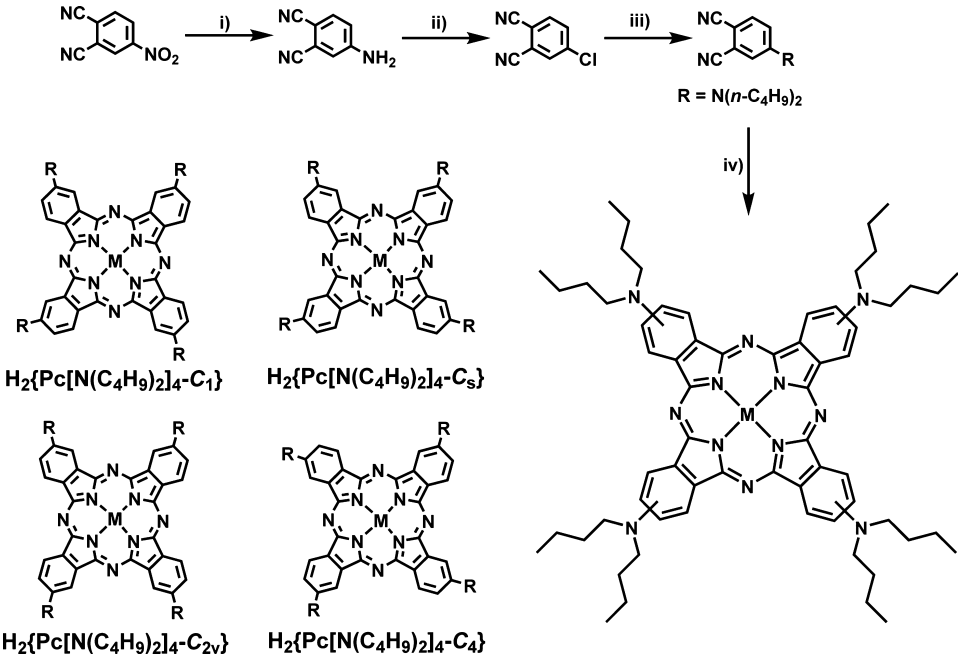

[a](i) Fe, HCl, CH_3OH, reflux; (ii) first $NaNO_2$, HCl, 0 °C; then CuCl, HCl, toluene, 80 °C; (iii) $HN(C_4H_9)_2$, K_2CO_3, DMF, 140 °C; (iv) for M = Mg, Mg, I_2, n-$C_5H_{11}OH$, reflux; for M = 2H, MgPc, CF_3COOH, rt; for M = Ni, Cu, and Zn, **1**, $M(OAc)_2{\cdot}H_2O$, DBU, n-$C_5H_{11}OH$, reflux.

and characterization of this series of tetrakis(dibutylamino)-phthalocyanine compounds by a series of spectroscopic methods including ^{1}H NMR spectroscopy with the help of hydrazine hydrate in CD_2Cl_2.

In the present paper, we describe the synthesis and spectroscopic and electrochemical properties of 2(3),9(10),16(17),23(24)-tetrakis(dibutylamino)-phthalocyanine compounds M{Pc[N(C_4H_9)$_2$]$_4$} (**1**−**5**; M = 2H, Mg, Ni, Cu, Zn; Scheme 1). Electrochemical studies revealed the significant shift in both the first oxidation and reduction potentials in the negative direction, even relative to those of M{Pc[N(C_4H_9)$_2$]$_8$}. Their lowest energy Q band also takes an obvious red shift in comparison with their octakis-(dibutylamino)phthalocyanine counterparts. This appears strange at first glance but is well rationalized by the more effective conjugation of the nitrogen lone pair of electrons in the dibutylamino side chains with the central phthalocyanine π system for the former species relative to the latter ones on the basis of structural and theoretical calculation results. This, in turn, results in superior nonlinear-optical (NLO) properties of H_2{Pc[N(C_4H_9)$_2$]$_4$} (**1**) over H_2{Pc[N(C_4H_9)$_2$]$_8$}, as revealed by the obviously larger effective imaginary third-order molecular hyperpolarizability (Im{$\chi^{(3)}$}) of 6.5 × 10^{-11} esu for the former species than the latter one with a value of 3.4 × 10^{-11} esu.

At the end of this section, it is worth noting that some phthalocyanine derivatives have been found to exhibit efficient second-order and, in particular, third-order NLO effects owing to their large polarizable π-conjugated system, showing application potential in optical limiting, optical computing, and optical communication.[12] This is surely true for the present phthalocyanine compounds. However, in the present case, investigation of the application-related third-order molecular hyperpolarizability of **1** in a comparative manner with that of H_2{Pc[N(C_4H_9)$_2$]$_8$} clearly reveals the structure−property relationship for the alkylamino-substituted phthalocyanines. Nevertheless, it must be pointed out that, despite the great efforts paid toward revealing the direct relationship between the peripheral substituents and photo/electric/magnetic functionalities for phthalocyanine materials, most results in this field still remain at the stage of realizing the connection of substituents with functionality-related electronic/spectroscopic/electrochemical properties. As a consequence, the present result seems to represent the first effort toward directly connecting the peripheral functional substituents, electronic structure, and NLO functionality together for phthalocyanine molecular materials, which will surely be helpful for the future development of functional phthalocyanine materials via molecular design and synthesis even through only tuning of the peripheral functional groups.

RESULTS AND DISCUSSION

Synthesis and Spectroscopic Characterization. The key precursor for the synthesis of tetrakis(dibutylamino)-phthalocyanine compounds, 4-(dibutylamino)phthalonitrile, was prepared[13] in three steps starting from 4-nitrophthalonitrile with an overall yield of 28.7% (Scheme 1). Despite the relatively low melting point for this compound associated with its peripheral bulky and long dibutylamino side chain, 44−46 °C, single crystals of 4-(dibutylamino)phthalonitrile suitable for X-ray diffraction analysis were fortunately obtained by evaporating its methanol/dichloromethane (1:1) solution to almost dryness at 0 °C. Interestingly, by means of a similar method, single crystals of 4,5-bis(dibutylamino)phthalonitrile suitable for X-ray diffraction analysis were also afforded by evaporating its dichloromethane solution at 0 °C and rendering X-ray diffraction analysis for this compound also possible for the first time. Figure 1 shows the molecular structure of 4-(dibutylamino)phthalonitrile. For comparative reasons, the

DOI: 10.1021/acs.inorgchem.6b00100
Inorg. Chem. XXXX, XXX, XXX−XXX

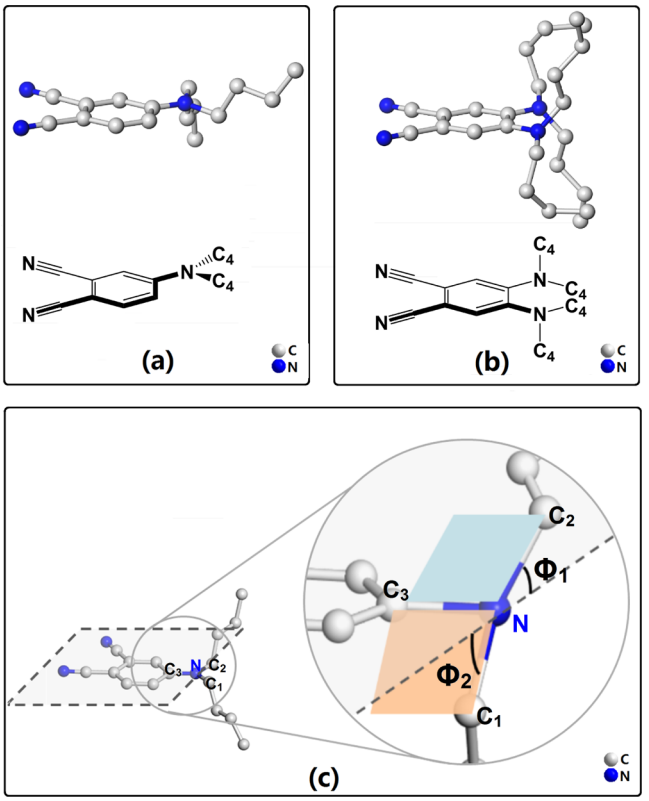

Figure 1. Molecular structures of 4-(dibutylamino)phthalonitrile (a) and 4,5-bis(dibutylamino)phthalonitrile (b) with the dihedral angle between the benzene plane and the plane determined by the carbon atom in the benzene moiety that connects to the nitrogen atom, the nitrogen atom, and the carbon atom neighboring to the nitrogen atom in the side chain, Φ_1 and Φ_2 (c). All of the hydrogen atoms have been omitted for clarity.

molecular structure of 4,5-bis(dibutylamino)phthalonitrile is also displayed in the same figure. According to diffraction analysis, the length of the C−N bond that links the benzene moiety and dibutylamino group for 4-(dibutylamino)-phthalonitrile amounts to 1.363 Å, which is significantly shorter than those in 4,5-bis(dibutylamino)phthalonitrile with values of 1.392 and 1.395 Å, suggesting much stronger interaction between the dibutylamino group and benzene moiety in the former species due to the more effective p−π conjugation between the nitrogen lone pair of electrons and the benzene moiety than that in 4,5-bis(dibutylamino)phthalonitrile. This is further clearly rationalized on the basis of the much smaller dihedral angles between the benzene plane and the plane determined by the carbon atom in the benzene moiety that connects to the nitrogen atom, the nitrogen atom, and the carbon atom neighboring to the nitrogen atom in the side chain(s), Φ_1 and Φ_2, for 4-(dibutylamino)phthalonitrile, 3.98 and 7.98°, relative to those for 4,5-bis(dibutylamino)-phthalonitrile, 18.42−18.95° and 55.08−55.88°, respectively (Figure 1 and Table S4 in the Supporting Information (SI).

Cyclic tetramerization of 4-(dibutylamino)phthalonitrile in refluxing *n*-pentanol in the presence of magnesium pentanoate led to the isolation of Mg{Pc[N(C_4H_9)$_2$]$_4$} (**2**) in a yield of 28.1%. Further treatment of **2** yielded in situ with trifluoro-acetic acid without the necessary isolation induced isolation of the corresponding metal free phthalocyanine **1** in a yield of 19.8%. The reaction of **1** with M(OAc)$_2$·H_2O (M = Ni, Cu, Zn) in refluxing *n*-pentanol and 1,8-diazabicyclo[5.4.0]undec-7-ene (DBU) afforded the corresponding phthalocyaninatometal complexes M{Pc[N(C_4H_9)$_2$]$_4$} (**3**−**5**; M = Ni, Cu, Zn) in yields of 50.3−57.9%. Satisfactory elemental analysis results were obtained for all of the newly prepared phthalocyanine derivatives **1**−**5** after repeated column chromatography followed by recrystallization. Their matrix-assisted laser desorption ionization time-of-flight (MALDI-TOF) MS spectra clearly show intense signals for the molecular ion M^+, which closely resemble the simulated ones, as shown in Figure S1 in the SI. These newly prepared phthalocyanine derivatives have also been characterized by other spectroscopic methods including ^{1}H NMR, electronic absorption, and IR spectroscopies.

The ^{1}H NMR spectra for compounds **1**−**3** and **5** containing either no metal ion or diamagnetic metal ion were recorded in CD_2Cl_2 in the presence of ca. 1% (v/v) hydrazine hydrate, which was used to reduce the small fraction of paramagnetic species to the neutral ones because of the easy oxidation nature of these compounds, in particular in solution as detailed below. Because of the paramagnetic nature of the divalent copper ion, the ^{1}H NMR spectrum could not be recorded for the copper complex **4** even with the help of hydrazine hydrate. As shown in Figure S2 in the SI, the three groups of aromatic protons due to the eight α protons and four β protons of the Pc ring in **1** give multiple signals at 8.97−8.85, 8.42−8.35, and 7.39−7.30 ppm with an integral ratio of 1:1:1, while the methylene, methylene, methylene, and methyl protons in the peripheral butyl groups give multiple signals at 3.75−3.72, 1.95−1.92, 1.64−1.62, and 1.20−1.14 ppm with an integral ratio of 2:2:2:3. This is also true for the metal complexes M{Pc[N(C_4H_9)$_2$]$_4$} (**2**, **3**, and **5**; M = Mg, Ni, Zn; Table S2 in the SI), except the

Table 1. Electronic Absorption Data for M{Pc[N(C_4H_9)$_2$]$_4$} (M = 2H, Mg, Ni, Cu, Zn), MPc (M = 2H, Zn), and M{Pc[N(C_4H_9)$_2$]$_8$} (M = 2H, Zn) in $CHCl_3$

compound	λ_{max}, nm (log ε, M^{-1} cm^{-1})					
1	340 (4.86)	463 (4.54)	517 (4.47)	681 (4.56)		765 (5.08)
H_2Pc[N(C_4H_9)$_2$]$_8$[a]	341 (4.94)		525 (4.64)		725 (5.08)	750 (5.17)
H_2Pc[b]	340 (4.99)				656 (5.15)	692 (5.22)
2	362 (5.04)	462 (4.42)	513 (4.37)	672 (4.61)		751 (5.24)
3	325 (4.99)	459 (4.49)	508 (4.34)	664 (4.53)		744 (5.15)
4	334 (4.98)	459 (4.51)	515 (4.46)	672 (4.64)		755 (5.23)
5	336 (4.91)	463 (4.36)	513 (4.43)	674 (4.61)		755 (5.23)
Zn{Pc[N(C_4H_9)$_2$]$_8$}[a]	341 (5.00)		522 (4.56)	657 (4.59)		732 (5.37)
ZnPc[b]	345 (4.52)			609 (4.30)		674 (5.13)

[a]Cited from ref 11. [b]Cited from ref 15.

DOI: 10.1021/acs.inorgchem.6b00100
Inorg. Chem. XXXX, XXX, XXX−XXX

lack of signals due to the inner isoindole protons. Because of the effective p−π conjugation between the peripheral nitrogen atoms and the central phthalocyanine chromophore, the ring current of **1** becomes smaller than that in $H_2Pc(^tBu)_4$, resulting in the observation of two inner isoindole proton signals for the former compound at a relatively lower field of 0.32−0.16 ppm in comparison with that at −2.17 ppm for the latter species.[14] At the end of this paragraph, it is worth noting that the mixture nature of the series of 2(3),9(10),16(17),23(24)-tetrakis-(dibutylamino)phthalocyanine compounds $M\{Pc[N(C_4H_9)_2]_4\}$ (**1**−**3** and **5**; M = 2H, Mg, Ni, Zn; each of which is composed of four regioisomers, as shown in Scheme 1) results in the multiplicity for all of the proton signals in their NMR spectra. This is actually also responsible for the relatively broadened absorption bands and redox peaks, as revealed in their electronic absorption spectra and cyclic voltammetry (CV) curves detailed below.

The electronic absorption spectra of **1**−**5** were recorded in $CHCl_3$, and the data are summarized in Table 1. As shown in Figure 2, **1** shows a typical nonaggregated molecular electronic

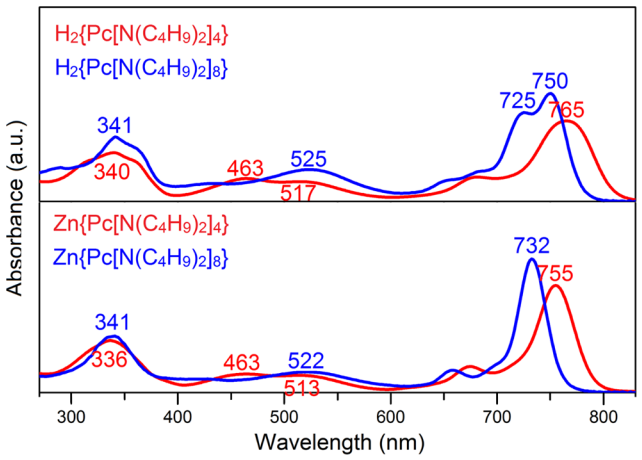

Figure 2. Comparison in the electronic absorption spectra between **1** (red) and $H_2\{Pc[N(C_4H_9)_2]_8\}$ (blue) as well as **5** (red) and $Zn\{Pc[N(C_4H_9)_2]_8\}$ (blue) in $CHCl_3$.

absorption spectrum of the metal-free phthalocyanines with a relatively broadened Soret absorption band appearing at 340 nm and a broad Q band at 765 nm. Interestingly, unlike the case of $H_2Pc(^tBu)_4$,[14] the Q band for **1** does not get split because of the effective p−π conjugation between the peripheral nitrogen atoms and the central phthalocyanine chromophore for the latter species, which, in turn, extends the effective conjugation system for this compound. It is worth noting that the band at 463−517 nm is due to the n → π* transitions arising from the nitrogen lone pair of electrons. Insertion of a metal ion into the phthalocyanine central core induces an increase in the molecular symmetry from D_{2h} for the central tetrapyrrole core of **1** to D_{4h} for $M\{Pc[N(C_4H_9)_2]_4\}$ (**2**−**5**; M = Mg, Cu, Ni, Zn), resulting in a significantly narrowed Q band in the range of 744−755 nm for these four metal complexes (Figure S6 in the SI and Table 1). In particular, in a comparison with $M\{Pc[N(C_4H_9)_2]_8\}$ (M = 2H, Mg, Cu, Zn), the Q absorption band for **1**−**5** takes a significant red shift (15−24 nm in the Q-band region), revealing the more extended conjugation system of $M\{Pc[N(C_4H_9)_2]_4\}$ than $M\{Pc[N(C_4H_9)_2]_8\}$. This, in turn, suggests the more effective conjugation of the nitrogen lone pair of electrons in the dibutylamino side chains with the central phthalocyanine π system for the former species relative to the latter one.

Figure S7 in the SI displays the IR spectra of **1**−**5**. As can be found, in addition to the absorption bands that are contributed from the central aromatic Pc macrocycle including the wagging and torsion vibrations of the C−H groups, isoindole ring stretching vibrations, and the C═N aza group stretching vibrations,[16] the absorptions observed at ca. 1090−1024 cm^{-1} are attributed to the C−N stretching vibrations of the $-N(C_4H_9)_2$ groups. The intense absorption bands observed at ca. 2954−2858 cm^{-1} in the IR spectra are the C−H stretching vibrations of the $-CH_2-$ and $-CH_3$ groups of the side chains. In the IR spectrum of **1**, a weak band at ca. 3291 cm^{-1} can be assigned to the N−H stretching vibrations of the isoindole moieties, which disappear in the IR spectra of the metal complexes $M\{Pc[N(C_4H_9)_2]_4\}$ (**2**−**5**; M = Mg, Ni, Cu, Zn).

Electrochemical Properties. The electrochemical behavior of **1**−**5** was investigated by CV in CH_2Cl_2 containing 0.1 M $[NBu_4][ClO_4]$. The half-wave potentials are summarized in Table 2. Figure 3 displays the cyclic voltammogram of

Table 2. Comparison in the Electrochemical Data between 1−5 and $M\{Pc[N(C_4H_9)_2]_8\}$ (M = 2H, Mg, Cu, Zn)

compound	Oxd_2	Oxd_1	Red_1	Red_2	ref
1	+0.73	+0.26	−1.03	−1.40	this work
$H_2\{Pc[N(C_4H_9)_2]_8\}$		+0.51	−0.89	−1.27	11
2	+0.56	+0.10	−1.38		this work
$Mg\{Pc[N(C_4H_9)_2]_8\}$		+0.088	−1.36		11
3	+0.78	+0.20	−1.10		this work
4	+0.76	+0.21	−1.13		this work
$Cu\{Pc[N(C_4H_9)_2]_8\}$		+0.29	−1.16		11
5	+0.53	+0.068	−1.35		this work
$Zn\{Pc[N(C_4H_9)_2]_8\}$		+0.10	−1.26		11

$Cu\{Pc[N(C_4H_9)_2]_4\}$ (**4**) as a typical representative. As can be seen, **4** exhibited two one-electron-like ligand-based oxidations at 0.76 and 0.21 V and one one-electron-like ligand-based reduction at −1.13 V with relatively broadened peak width in comparison with that of the octakis-(dibutylamino)phthalocyanine counterparts[11] because of its four-regioisomer-containing mixture nature. As can be seen in Figure 3, linear convolution integral (LCI) analysis clearly gives four individual peaks for the first oxidation process of **4** due to the four regioisomers of this compound.[17] This is surely also true for the remaining redox processes of this compound and remaining members of the whole series (Table SS2 in the SI). In addition, a comparison of the corresponding electrochemical properties between $M\{Pc[N(C_4H_9)_2]_4\}$ and $M\{Pc[N-(C_4H_9)_2]_8\}$ indicates that the introduction of four dibutylamino groups onto the peripheral positions of the phthalocyanine chromophore induces a significant shift in both the first oxidation and reduction potentials in the negative direction, relative to those of octakis(dibutylamino)phthalocyanine counterparts.[11] This is truly strange at first glance but fortunately well rationalized by the more effective conjugation of the nitrogen lone pair of electrons in the dibutylamino side chains with the central phthalocyanine π system for the former species relative to the latter ones on the basis of structural and theoretical calculation as detailed below. At the end of this section, it is worth noting that the first oxidation potentials for $M\{Pc[N(C_4H_9)_2]_4\}$ (**1**−**5**; M = 2H, Mg, Ni, Cu, Zn) and

DOI: 10.1021/acs.inorgchem.6b00100
Inorg. Chem. XXXX, XXX, XXX−XXX

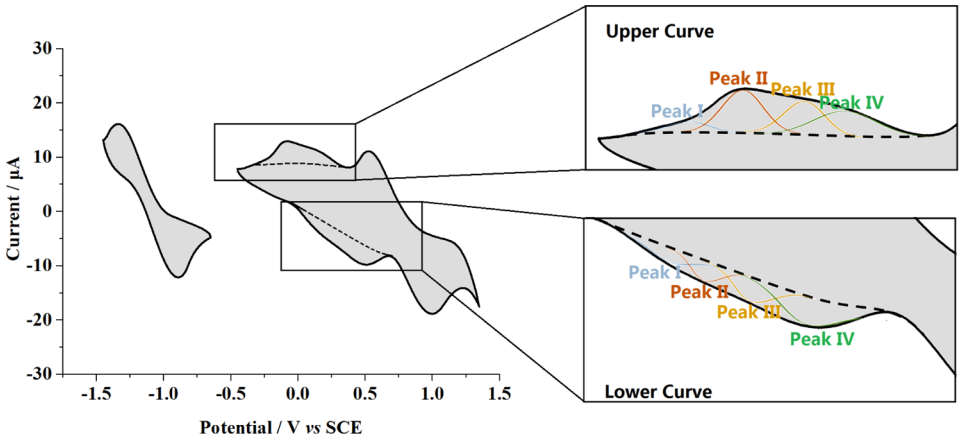

Figure 3. Cyclic voltammogram of **4** in CH_2Cl_2 containing 0.1 M $[NBu_4][ClO_4]$ at a scan rate of 30 mV s^{-1} together with its LCI analysis.

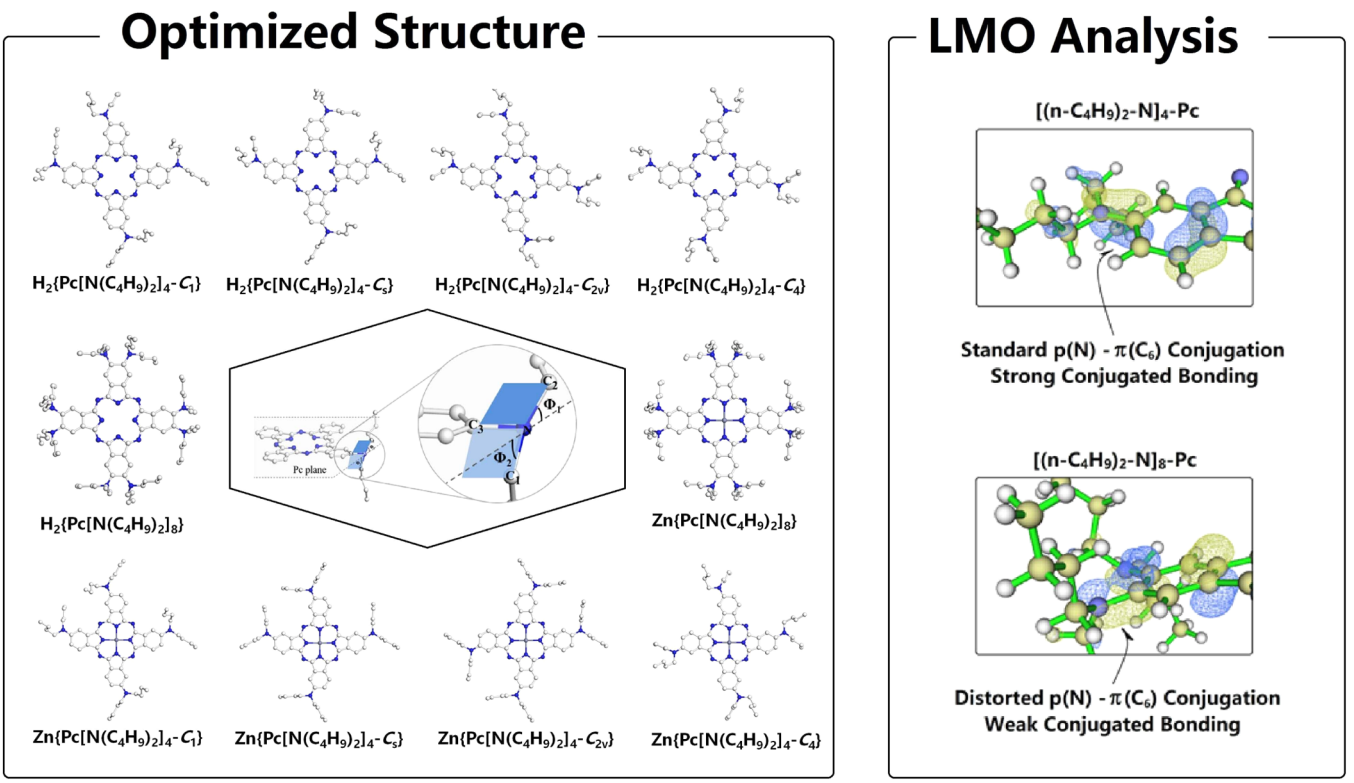

Figure 4. Simulated molecular structures and LMO analysis for $M\{Pc[N(C_4H_9)_2]_4\}$ and $M\{Pc[N(C_4H_9)_2]_8\}$ (M = 2H, Zn).

$M\{Pc[N(C_4H_9)_2]_8\}$ (M = 2H, Mg, Cu, Zn) locate in the ranges of +0.068 to +0.26 and +0.088 to +0.51 eV, respectively, indicating the easier oxidation of the four dibutylamino-substituted phthalocyanines (or at least one of the four regioisomers) than the eight dibutylamino-substituted counterparts. This, in turn, becomes responsible for the quite high instability of the former species in particular in solutions. As mentioned above, satisfied ^{1}H NMR spectra for **1**−**3** and **5** could only be obtained with the help of hydrazine hydrate.

Density Functional Theory (DFT) Investigation. In order to gain insight into the electronic structures and electronic absorption spectra of these newly prepared phthalocyanine compounds, DFT calculation over $M\{Pc[N(C_4H_9)_2]_4\}$ (M = 2H, Zn) was carried out using B3LYP for molecular optimization and τHCTHhyb for the simulation of transition spectra.[18] A mixed basis set, including 6-31G(d) for carbon/hydrogen/nitrogen and LanL2DZ for zinc, was employed to describe the wave function.[19] For the purposes of comparison, those for $M\{Pc[N(C_4H_9)_2]_8\}$ (M = 2H, Zn) have also been calculated at the same level. It is worth mentioning that, because of the lack of single-crystal structures for $M\{Pc[N(C_4H_9)_2]_4\}$, the simulated ones were employed for further theoretical studies. Fortunately, such a fact that the simulated structures for $M\{Pc[N(C_4H_9)_2]_8\}$ (M = 2H, Zn) correspond well with their single-crystal molecular structures ensures the validity of the present treatment. Additional support for this point comes from the good accordance in the two dihedral angles, Φ_1 and Φ_2, revealed by single-crystal X-ray diffraction analysis for 4-(dibutylamino)phthalonitrile with the calculated ones for $M\{Pc[N(C_4H_9)_2]_4\}$ (M = 2H, Zn) vide infra.

DOI: 10.1021/acs.inorgchem.6b00100
Inorg. Chem. XXXX, XXX, XXX−XXX

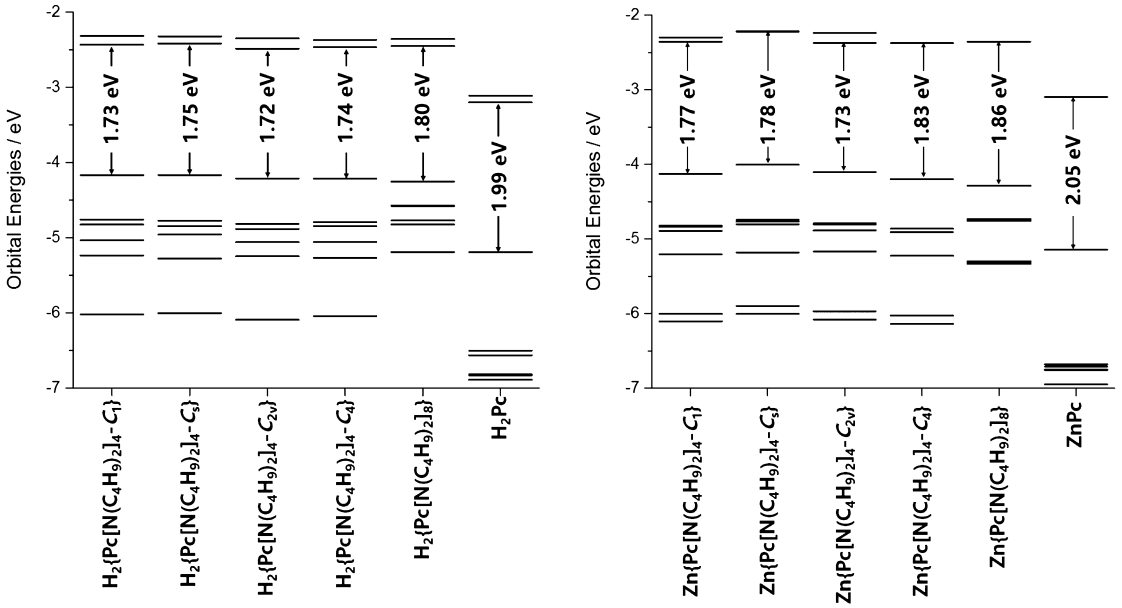

Figure 5. Molecular orbital energies of MPc, M{Pc[N(C_4H_9)$_2$]$_4$}, and M{Pc[N(C_4H_9)$_2$]$_8$} (M = 2H, Zn).

The optimized structures of M{Pc[N(C_4H_9)$_2$]$_4$} including M{Pc[N(C_4H_9)$_2$]$_4$-C_4}, M{Pc[N(C_4H_9)$_2$]$_4$-C_1}, M{Pc[N-(C_4H_9)$_2$]$_4$-C_s}, and M{Pc[N(C_4H_9)$_2$]$_4$-C_{2v}} together with M{Pc[N(C_4H_9)$_2$]$_8$} (M = 2H, Zn) are shown in Figure 4. As can be found, the distorted degree between the peripheral −N(C_4H_9)$_2$ substituents and the central Pc macrocycle can be measured by two key dihedral angles, Φ_1 and Φ_2 (Figure 4 and Table S5 in the SI). For M{Pc[N(C_4H_9)$_2$]$_4$} (M = 2H, Zn), DFT calculation results reveal that Φ_1 and Φ_2 locate in the ranges of 1−7° and 3−25°, respectively. These data are in good accordance with those found in 4-(dibutylamino)phthalonitrile by X-ray diffraction analysis (Figure 1 and Table S3 in the SI). However, the steric hindrance between the two dibutylamino groups at the neighboring peripheral positions of the phthalocyanine skeleton for M{Pc[N(C_4H_9)$_2$]$_8$} (M = 2H, Zn) leads to an increase in both Φ_1 and Φ_2 to 23−26° and 56−58°, which are in line with the experimental findings for both 4,5-bis(dibutylamino)phthalonitrile and M{Pc[N(C_4H_9)$_2$]$_8$} (M = 2H, Zn).[11] These results obviously suggest the more effective p−π conjugation between the dibutylamino nitrogen atoms and the central phthalocyanine chromophore in the former tetrakis(dibutylamino)phthalocyanines in comparison with that in the latter octakis(dibutylamino)phthalocyanine counterparts, which is further revealed by the local molecular orbital (LMO) analysis[20] (Figure 4). For the purpose of further disclosing the p−π conjugating strength in a quantitative manner, the Mayer bond order analysis[21] for both M{Pc[N-(C_4H_9)$_2$]$_4$} and M{Pc[N(C_4H_9)$_2$]$_8$} (M = 2H, Zn) is carried out. According to the calculating result, the total π(N−C) bond order between the peripheral −N(C_4H_9)$_2$ substituents and the central Pc macrocycle amounts to 0.449 for M{Pc[N-(C_4H_9)$_2$]$_4$}, which is only 0.155 for M{Pc[N(C_4H_9)$_2$]$_8$}.

In order to differentiate the effect of four peripheral dibutylamino substituents from eight at the phthalocyanine periphery, the molecular orbitals for MPc, M{Pc[N(C_4H_9)$_2$]$_4$}, and M{Pc[N(C_4H_9)$_2$]$_8$} (M = 2H, Zn) have been calculated in a comparative manner. As can be clearly seen in Figure 5 and Table S9 in the SI, incorporation of the electron-donating dibutylamino substituents onto the peripheral positions of phthalocyanine leads to an obvious increase in the HOMO from −5.19 eV for H_2Pc to (−4.21)−(−4.16) eV for **1** and −4.25 eV for H_2{Pc[N(C_4H_9)$_2$]$_8$} and the lowest unoccupied molecular orbital (LUMO) energy level from −3.20 eV for H_2Pc to (−2.42)−(−2.49) eV for **1** and −2.5 eV for H_2{Pc[N(C_4H_9)$_2$]$_8$}. Interestingly, four peripheral dibutylamino substituents introduced are more effective than eight in elevating the HOMO and LUMO energy levels of the phthalocyanine system because of the much more effective p−π conjugation in **1** than in H_2{Pc[N(C_4H_9)$_2$]$_8$}. This is also true for the phthalocyaninatozinc complexes (Figure 5). These results appear to be in line with the experimental data, as revealed by the electrochemical method detailed above.

In order to clarify the effect of phthalocyanine peripheral dibutylamino substituents on the electronic absorption spectra, the electron transition properties for M{Pc[N(C_4H_9)$_2$]$_4$} and M{Pc[N(C_4H_9)$_2$]$_8$} (M = Zn, 2H) are carried out using time-dependent DFT calculation. As can be found in Tables S7 and S8 in the SI, the electronic absorption spectra in the range of 400−800 nm can be divided into two regions including region I (600−800 nm) and region II (400−600 nm) based on the different electron transition models. For **1**, the absorption in region I (600−800 nm) originates from the transition from HOMO to LUMO/LUMO+1. The energy gap between HOMO and LUMO/LUMO+1 for H_2Pc is 1.99/2.08 eV (Figure 5). However, the introduction of four electron-donating −N(C_4H_9)$_2$ substituents results in a significant decrease in the HOMO and LUMO/LUMO+1 energy gap to 1.73/1.85, 1.75/1.84, 1.72/1.89, and 1.74/1.84 eV for H_2{Pc-[N(C_4H_9)$_2$]$_4$-C_1}, H_2{Pc[N(C_4H_9)$_2$]$_4$-C_s}, H_2{Pc[N(C_4H_9)$_2$]$_4$-C_{2v}}, and H_2{Pc[N(C_4H_9)$_2$]$_4$-C_4}, respectively, mainly because of the effective p−π conjugation between the peripheral −N(C_4H_9)$_2$ substituents and the central Pc macrocycle. This, in turn, induces a significant red shift in the phthalocyanine Q bands of **1** relative to those of H_2Pc, with 718/681 nm for H_2{Pc[N(C_4H_9)$_2$]$_4$-C_1}, 701/695 nm for H_2{Pc[N(C_4H_9)$_2$]$_4$-C_s}, 729/672 nm for H_2{Pc[N(C_4H_9)$_2$]$_4$-C_{2v}}, and 704/690 nm for H_2{Pc[N(C_4H_9)$_2$]$_4$-C_4} to 598/594 nm for H_2Pc. It is worth mentioning that overlapping of the Q bands for the four isomers leads to a relatively broadened Q band as a whole, as observed for H_2{Pc[N(C_4H_9)$_2$]$_4$} by UV−vis spectrometry. This

DOI: 10.1021/acs.inorgchem.6b00100
Inorg. Chem. XXXX, XXX, XXX−XXX

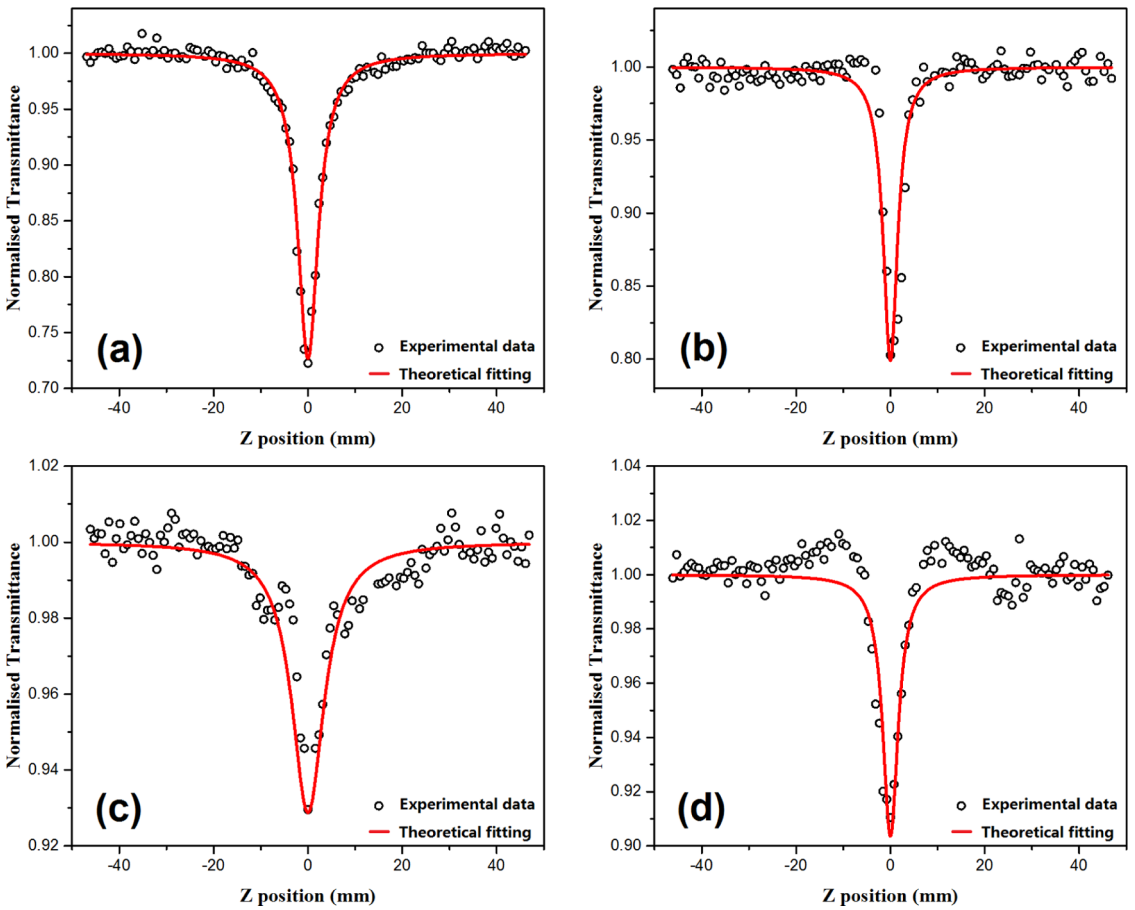

Figure 6. Open-aperture *Z*-scan traces of **1** (a), $H_2\{Pc[N(C_4H_9)_2]_8\}$ (b), $H_2[Pc(OC_5H_{11})_8]$ (c), and $H_2Pc(^tBu)_4$ (d) in toluene with theoretical fitting curves.

is surely also true for $Zn\{Pc[N(C_4H_9)_2]_4\}$ (**5**; Table S8 in the SI). Because of the lack of effective p−π conjugation between the peripheral $-N(C_4H_9)_2$ substituents and the central Pc macrocycle in the octakis(dibutylamino)phthalocyanine compounds as detailed above, the incorporation of eight dibutylamino groups onto the phthalocyanine periphery leads to a lesser degree of decrease in the HOMO and LUMO/LUMO+1 energy gap to 1.99/2.08 eV, which, in turn, results in a lesser degree of red-shifted Q bands from 598/594 nm for H_2Pc to 689/678 nm for $H_2\{Pc[N(C_4H_9)_2]_8\}$ (Tables S6 and S7 in the SI). These results are in line with the experimental findings.

The bands of region II (400−600 nm) for $M\{Pc[N(C_4H_9)_2]_4\}$ (M = Zn, 2H) mainly come from the transition from HOMO−4 to LUMO/LUMO+1. As can be found in Table S8 in the SI, the starting orbital HOMO−4 distributes at both the peripheral $-N(C_4H_9)_2$ substituents and the central Pc macrocycle, revealing the coupled orbital nature of this orbital due to the p$[-N(C_4H_9)_2]-\pi$(Pc) conjugation. On the basis of the photon-induced electron-transfer analysis[22] (Table S8 in the SI), the broad absorption band in region II (400−600 nm) for **1** is induced by the electron density movements from the peripheral substituent to the central macrocycle along with the electron pathway constructed by p−π conjugation, indicating the origination of this new absorption band associated with the introduction of the peripheral conjugated system. This is also true for **5** (Table S8 in the SI).

NLO Properties. The third-order NLO properties of **1** and $H_2\{Pc[N(C_4H_9)_2]_8\}$ in toluene at a concentration of 1.0×10^{-4} mol L^{-1} were studied using the *Z*-scan technique with a Nd:YAG laser as the light source (a pulse width of 8 ns and a wavelength of 532 nm).[23] For comparative purposes, those of $H_2Pc(^tBu)_4$ and $H_2[Pc(OC_5H_{11})_8]$ have also been investigated. In addition, measurement over pure toluene was also performed underexactly the same experimental conditions to verify the origination of the third-order NLO properties from the phthalocyanine material rather than from the solvent.

The NLO absorption components were obtained by the *Z*-scan experiment under an open-aperture configuration. As shown in Figure 6, both **1** and $H_2\{Pc[N(C_4H_9)_2]_8\}$ in toluene display reverse saturation absorption under an open-aperture configuration. According to the equations employed previously to well describe the third-order NLO absorption process,[24] the effective imaginary third-order molecular hyperpolarizability ($Im\{\chi^{(3)}\}$) for **1** was calculated to be 6.5×10^{-11} esu, which is significantly larger than that for $H_2\{Pc[N(C_4H_9)_2]_8\}$, 3.4×10^{-11} esu, because of the more extended conjugation system for the former species, as detailed above. In addition, even the effective imaginary third-order molecular hyperpolarizability ($Im\{\chi^{(3)}\}$) for $H_2\{Pc[N(C_4H_9)_2]_8\}$ was found to still be obviously larger than that of $H_2[Pc(OC_5H_{11})_8]$ and $H_2Pc(^tBu)_4$ with values of 2.2×10^{-11} and 8.2×10^{-12} esu, respectively, revealing the more electron-donating property of the $-N(C_4H_9)_2$ group than the OC_5H_{11} and ^{t}Bu groups.

DOI: 10.1021/acs.inorgchem.6b00100
Inorg. Chem. XXXX, XXX, XXX−XXX

CONCLUSION

In summary, 2(3),9(10),16(17),23(24)-tetrakis(dibutylamino)-phthalocyanine compounds have been prepared and spectroscopically characterized for the first time. Electrochemical measurement reveals the significantly raised HOMO and LUMO energy levels due to the effective p−π conjugation between the peripheral nitrogen atoms and phthalocyanine chromophore in comparison with their 2,3,9,10,16,17,23,24-octakis(dibutylamino)phthalocyanine counterparts. This, in turn, results in superior third-order NLO properties of **1** over $H_2\{Pc[N(C_4H_9)_2]_8\}$. This result directly connects the peripheral functional substituents, electronic structures, and NLO functionalities of phthalocyanine molecular materials together for the first time, opening a new way toward developing novel functional phthalocyanine materials via molecular design by relying upon the peripheral functional groups.

EXPERIMENTAL SECTION

General Procedures. 4-Nitrophthalonitrile was purchased from J&K Scientific Ltd. *n*-Pentanol was freshly distilled from sodium. *N*,*N*-Dimethylformamide (DMF) was freshly distilled from CaH_2. Column chromatography was carried out on silica gel (200−300 mesh) or alkaline alumina (200−300 mesh) with the indicated eluents. The electrolyte $[NBu_4][ClO_4]$ was recrystallized twice from tetrahydrofuran (THF). All other reagents and solvents were used as received.

^{1}H NMR spectra were recorded on a Bruker DPX 400 spectrometer in $CDCl_3$ or CD_2Cl_2/80% hydrazine hydrate (100:1, v/v). Spectra were referenced internally using the residual solvent resonance (7.26 ppm in $CDCl_3$ or 5.32 ppm in CD_2Cl_2 for ^{1}H NMR) relative to $SiMe_4$. Electronic absorption spectra were recorded on a Hitachi U-2910 spectrophotometer. IR spectra were recorded as KBr pellets using a Bruker Tensor 37 spectrometer with 2 cm^{-1} resolution. MALDI-TOF MS spectra were taken on a Bruker BIFLEX III ultrahigh-resolution Fourier transform ion cyclotron resonance mass spectrometer with α-cyano-4-hydroxycinnamic acid as the matrix. Elemental analyses were performed on an Elementar Vavio El III elemental analyzer. Electrochemical measurements were carried out with a BAS CV-50W voltammetric analyzer. The cell comprised inlets for a glassy-carbon-disk working electrode with a diameter of 2.0 mm and a silver-wire counter electrode. The reference electrode was Ag^+/Ag (a solution of 0.01 M $AgNO_3$ and 0.1 M TBAP in acetonitrile), which was connected to the solution by a Luggin capillary, whose tip was placed close to the working electrode. It was corrected for junction potentials by being referenced internally to the ferrocenium/ferrocene (Fc^+/Fc) couple [$E_{1/2}(Fc^+/Fc)$ = 0.501 V vs SCE]. Typically, a 0.1 M solution of $[NBu_4][ClO_4]$ in CH_2Cl_2 containing a 1 mM sample was purged with nitrogen for 10 min, and then the voltammograms were recorded at ambient temperature. Crystal data for 4-(dibutylamino)-phthalonitrile and 4,5- bis(dibutylamino)phthalonitrile were determined by X-ray diffraction analysis at 298 K using an Oxford Diffraction Gemini E system with Mo Kα radiation (λ = 0.71073 Å), and details of the structure refinement are given in Table S3 in the SI. CCDC 1442281 and 1442282 containing the supplementary crystallographic data for this paper can be obtained free of charge from the Cambridge Crystallographic Data Centre via www.ccdc.cam.ac.uk/data_request/cif.

Synthesis of 4-(Dibutylamino)phthalonitrile. To a mixture of 4-chlorophthalonitrile (6.70 g, 41.2 mmol) and K_2CO_3 (11.4 g, 82.5 mmol) in DMF (70 mL) at 140 °C was added dibutylamine (15.9 g, 124 mmol). The resulting system was heated at the same temperature for 18 h. After being cooled to room temperature, the reaction mixture was poured into water (200 mL), extracted with petroleum ether, dried over Na_2SO_4, and filtered. After the solvent was removed by evaporation under reduced pressure, the crude product was chromatographed on a silica gel column using dichloromethane/petroleum ether (1:1) as the eluent, giving the target compound as light-pink oil with a yield of 66.2% (6.97 g), which becomes a pink solid at temperatures below 0 °C. Single crystals of 4-(dibutylamino)-phthalonitrile suitable for X-ray diffraction analysis were obtained by evaporating its methanol/dichloromethane (1:1) solution to almost dryness at 0 °C. Mp: 44−46 °C. ^{1}H NMR ($CDCl_3$, 400 MHz): δ 7.48 (d, J = 9.00 Hz, 1 H), 6.83 (d, J = 2.20 Hz, 1 H), 6.74 (q, J = 3.76 Hz, 1 H), 3.31 (t, J = 7.74 Hz, 4 H), 1.56 (m, J = 7.63 Hz, 4 H), 1.37 (m, J = 7.49 Hz, 4 H), 0.97 (t, J = 7.30 Hz, 6 H).

*Synthesis of 2(3),9(10),16(17),23(24)-Tetrakis(dibutylamino)-phthalocyaninatomagnesium Mg{Pc[N(C_4H_9)$_2$]$_4$} (**2**).* A mixture of magnesium turnings (24.6 mg, 1.03 mmol) and a small amount of iodine in anhydrous *n*-pentanol (5 mL) were refluxed for 1 h under a slow steam of nitrogen. Then 4-(dibutylamino)phthalonitrile (522 mg, 2.04 mmol) was added. The resulting mixture was refluxed for another 24 h. After being cooled, the solvent was evaporated. The crude product was chromatographed on an alkaline alumina column with dichloromethane/methanol (100:2) as the eluent. Repeated column chromatography followed by recrystallization from THF and methanol gave a dark-green solid with a yield of 28.1% (150 mg). Elem anal. Calcd for $C_{64}H_{84}N_{12}Mg\cdot0.75CH_2Cl_2\cdot0.125C_4H_8O$: C, 70.07; H, 7.79; N, 15.03. Found: C, 69.99; H, 7.86; N, 15.09. ^{1}H NMR (CD_2Cl_2, 400 MHz): δ 9.12−8.93 (m, 4 H), 8.59−8.52 (m, 4 H), 7.42−7.36 (m, 4 H), 3.78−3.74 (m, 16 H), 1.98−1.91 (m, 16 H), 1.68−1.59 (m, 16 H), 1.17−1.13 (m, 24 H). MS (MALDI-TOF). Calcd for $C_{64}H_{84}N_{12}Mg$ [$(M)^+$]: m/z 1044.7. Found: m/z 1044.1. UV−vis [$CHCl_3$; λ, nm (log ε, $\times10^{-5}$ M^{-1} cm^{-1})]: 751 (1.74), 672 (0.404), 513 (0.237), 462 (0.263), 362 (1.09).

*Synthesis of 2(3),9(10),16(17),23(24)-Tetrakis(dibutylamino)-phthalocyanine H_2{Pc[N(C_4H_9)$_2$]$_4$} (**1**).* Compound **2** (117 mg, 0.112 mmol) was dissolved in CF_3COOH (3 mL) and stirred under a slow steam of nitrogen for 15 min. The reaction mixture was then poured into cold water and neutralized with an ammonia solution. The precipitate collected was washed several times with CH_3OH and then applied on an alkaline alumina column with dichloromethane as the eluent. Repeated chromatography followed by recrystallization from THF and methanol afforded the target compound as a dark-green solid with a yield of 70.5% (80.7 mg). Elem anal. Calcd for $C_{64}H_{86}N_{12}\cdot0.125CH_2Cl_2\cdot0.25H_2O$: C, 74.16; H, 8.42; N, 16.18. Found: C, 74.11; H, 8.24; N, 16.21. ^{1}H NMR (CD_2Cl_2, 400 MHz): δ 8.97−8.85 (m, 4 H), 8.42−8.35 (m, 4 H), 7.39−7.30 (m, 4 H), 3.75−3.72 (m, 16 H), 1.95−1.92 (m, 16 H), 1.64−1.62 (m, 16 H), 1.20−1.14 (m, 24 H), 0.32−0.16 (m, 2 H). MS (MALDI-TOF). Calcd for $C_{64}H_{86}N_{12}$ [$(M)^+$]: m/z 1022.7. Found: m/z 1022.9. UV−vis [$CHCl_3$; λ, nm (log ε, $\times10^{-5}$ M^{-1} cm^{-1})]: 765 (1.20), 681 (0.366), 517 (0.296), 463 (0.343), 340 (0.728).

*Synthesis of 2(3),9(10),16(17),23(24)-Tetrakis(dibutylamino)-phthalocyaninatonickel Ni{Pc[N(C_4H_9)$_2$]$_4$} (**3**).* A mixture of compound **1** (80.5 mg, 0.0787 mmol), $Ni(OAc)_2\cdot4H_2O$ (78.3 mg, 0.315 mmol), and DBU (0.5 mL) in anhydrous *n*-pentanol (3 mL) was heated to reflux for 10 h under nitrogen. After being cooled to room temperature, the mixture was evaporated to dryness under reduced pressure, and the residue was chromatographed on an alkaline alumina column using dichloromethane/methanol (200:1) as the eluent. Repeated chromatography followed by recrystallization from THF and methanol gave a dark-green sample with a yield of 50.6% (43.0 mg). Elem anal. Calcd for $C_{64}H_{84}N_{12}Ni\cdot0.75CH_2Cl_2$: C, 67.99; H, 7.53; N, 14.69. Found: C, 67.83; H, 7.58; N, 14.64. ^{1}H NMR (CD_2Cl_2, 400 MHz): δ 8.64−8.33 (m, 4 H), 8.11−7.86 (m, 4 H), 7.20−6.99 (m, 4 H), 3.65−3.57 (m, 16 H), 1.91−1.89 (m, 16 H), 1.64−1.61 (m, 16 H), 1.18−1.16 (m, 24 H). MS (MALDI-TOF). Calcd for $C_{64}H_{84}N_{12}Ni$ [$(M)^+$]: m/z 1078.6. Found: m/z 1078.5. UV−vis [$CHCl_3$; λ, nm (log ε, $\times10^{-5}$ M^{-1} cm^{-1})]: 744 (1.42), 664 (0.342), 508 (0.220), 459 (0.312), 325 (0.977).

*Synthesis of 2(3),9(10),16(17),23(24)-Tetrakis(dibutylamino)-phthalocyaninatocopper Cu{Pc[N(C_4H_9)$_2$]$_4$} (**4**).* When the procedure described above using $Cu(OAc)_2\cdot H_2O$ (62.8 mg, 0.315 mmol) instead of $Ni(OAc)_2\cdot4H_2O$ as the starting material was employed, compound **4** was obtained after repeated chromatography with dichloromethane/methanol (200:1) as the eluent, followed by recrystallization from THF and methanol, which gave a dark-green sample with a yield of 50.3% (43.0 mg). Elem anal. Calcd for $C_{64}H_{84}N_{12}Cu\cdot0.25CH_2Cl_2\cdot$

DOI: 10.1021/acs.inorgchem.6b00100
Inorg. Chem. XXXX, XXX, XXX−XXX

0.125H_2O·0.5CH_3OH: C, 69.16; H, 7.78; N, 14.95. Found: C, 69.13; H, 7.58; N, 14.89. MS (MALDI-TOF). Calcd for $C_{64}H_{84}N_{12}Cu$ [$(M)^+$]: m/z 1083.6. Found: m/z 1083.4. UV−vis [$CHCl_3$; λ, nm (log ε, $\times 10^{-5}$ M^{-1} cm^{-1})]: 755 (1.70), 672 (0.432), 508 (0.220), 459 (0.323), 334 (0.966).

Synthesis of 2(3),9(10),16(17),23(24)-Tetrakis(dibutylamino)-phthalocyaninatozinc Zn{Pc[N(C_4H_9)$_2$]$_4$} (5). When the above-described procedure used to prepare Ni{Pc[N(C_4H_9)$_2$]$_4$} (**3**) with $Zn(OAc)_2·2H_2O$ (69.1 mg, 0.315 mmol) instead of $Ni(OAc)_2·4H_2O$ as the starting material was employed, pure **5** was isolated as a dark-green sample with a yield of 57.9% (49.5 mg). Elem anal. Calcd for $C_{64}H_{84}N_{12}Zn·0.5CH_2Cl_2$: C, 68.60; H, 7.59; N, 14.88. Found: C, 68.44; H, 7.58; N, 14.83. ^{1}H NMR (CD_2Cl_2, 400 MHz): δ 9.13−9.09 (t, 4 H), 8.60−8.59 (d, 4 H), 7.44−7.43 (d, 4 H), 3.78−3.75 (t, 16 H), 1.98−1.90 (m, 16 H), 1.66−1.61 (m, 16 H), 1.17−1.14 (t, 24 H). MS (MALDI-TOF). Calcd for $C_{64}H_{84}N_{12}Zn$ [$(M)^+$]: m/z 1084.6. Found: m/z 1084.5. UV−vis [$CHCl_3$; λ, nm (log ε, $\times 10^{-5}$ M^{-1} cm^{-1})]: 755 (1.68), 674 (0.407), 513 (0.269), 463 (0.230), 336 (0.815).

■ ASSOCIATED CONTENT

Supporting Information

The Supporting Information is available free of charge on the ACS Publications website at DOI: 10.1021/acs.inorgchem.6b00100.

Validity of the functional τHCTHhyb and a systematic comparison between the cyclic voltammograms for M{Pc[N(C_4H_9)$_2$]$_4$} and M{Pc[N(C_4H_9)$_2$]$_8$}, experimental and simulated isotopic patterns for **1**−**5**, ^{1}H NMR spectrum of **1**−**3** and **5**, electronic absorption and IR spectra of **1**−**5**, cyclic voltammograms of **1**−**5**, analytical and MS data for **1**−**5**, ^{1}H NMR data (δ) for **1**−**3** and **5**, crystal data and structure refinements for 4-(dibutylamino)phthalonitrile and 4,5-bis(dibutylamino)-phthalonitrile, two dihedral angles, Φ_1 and Φ_2, for 4-(dibutylamino)phthalonitrile, 4,5-bis(dibutylamino)-phthalonitrile, M{Pc[N(C_4H_9)$_2$]$_4$} (M = 2H, Zn), and M{Pc[N(C_4H_9)$_2$]$_8$} (M = 2H, Zn), electron density difference plots of electron transitions and molecular orbital maps for MPc (M = 2H, Zn), M{Pc[N(C_4H_9)$_2$]$_8$} (M = 2H, Zn), and M{Pc[N(C_4H_9)$_2$]$_4$} (M = 2H, Zn) (PDF)

X-ray crystallographica data in CIF format (CIF)

X-ray crystallographica data in CIF format (CIF)

■ AUTHOR INFORMATION

Corresponding Authors

*E-mail: qdd@ustb.edu.cn (D.Q.).

*E-mail: jianzhuang@ustb.edu.cn (J.J.).

Notes

The authors declare no competing financial interest.

■ ACKNOWLEDGMENTS

Financial support from the National Key Basic Research Program of China (Grants 2012CB224801 and 2013CB933402), National Natural Science Foundation of China (Grants 21290174, 21301017, and 21401009), and Beijing Municipal Commission of Education is gratefully acknowledged.

■ REFERENCES

(1) (a) Lever, A. B. P., Leznoff, C. C., Eds. *Phthalocyanine: Properties and Applications*; VCH: New York, 1989−1996; Vols. *1*−*4*. (b) McKeown, N. B. *Phthalocyanines Materials: Synthesis, Structure and Function*; Cambridge University Press: New York, 1998. (c) Kadish, K. M., Smith, K. M., Guilard, R., Eds. *The Porphyrin Handbook*; Academic Press: San Diego, CA, 2000 and 2003; Vols. *1*−*20*. (d) Mingos, D. M. P., Jiang, J., Eds. *Functional Phthalocyanine Molecular Materials, Structure and Bonding*; Springer-Verlag: Heidelberg, Germany, 2010; Vol. *135*.

(2) (a) Rosenthal, I.; Ben-Hur, E. *Int. J. Radiat. Biol.* **1995**, *67*, 85−91. (b) Bonnett, R. *Chem. Soc. Rev.* **1995**, *24*, 19−33. (c) Dutta, S.; Ongarora, B. G.; Li, H.; Vicente, M. D. G. H.; Kolli, B. K.; Chang, K. P. *PLoS One* **2011**, *6*, e20786.

(3) (a) Gregory, P. *High-Technology Applications of Organic Colorants*; Plenum Press: New York, 1991. (b) Ao, R.; Kümmerl, L.; Haarer, D. *Adv. Mater.* **1995**, *7*, 495−499. (c) Birkett, D. *Chem. Ind.* **1997**, *5*, 178−181.

(4) (a) Wohrle, D.; Schlettwein, D.; Schnurpfeil, G.; Schneider, G.; Karmann, E.; Yoshida, T.; Kaneko, M. *Polym. Adv. Technol.* **1995**, *6*, 118−130. (b) Calvete, M. J. F.; Silva, M.; Pereira, M. M.; Burrows, H. D. *RSC Adv.* **2013**, *3*, 22774−22789. (c) Xing, R.; Wu, L.; Fei, Z.; Wu, P. *J. Mol. Catal. A: Chem.* **2013**, *371*, 15−20. (d) Zhang, Z.; Wang, W.; Zhang, L. *Dalton. Trans.* **2013**, *42*, 4579−4585. (e) Yamamoto, A.; Teramura, K.; Hosokawa, S.; Shishido, T.; Tanaka, T. *ChemCatChem* **2015**, *7*, 1818−1825.

(5) (a) Song, F.; Wells, J. W.; Handrup, K.; Li, Z. S.; Bao, S. N.; Schulte, K.; Ahola-Tuomi, M.; Mayor, L. C.; Swarbrick, J. C.; Perkins, E. W.; Gammelgaard, L.; Hofmann, P. *Nat. Nanotechnol.* **2009**, *4*, 373−376. (b) Lu, H.; Kwak, I.; Park, J. H.; O'Neill, K.; Furuyama, T.; Kobayashi, N.; Seabaugh, A.; Kummel, A.; Fullerton-Shirey, S. K. *J. Phys. Chem. C* **2015**, *119*, 21992−22000.

(6) (a) Divay, L.; Barny, P.; Loiseaux, B.; Delaire, J. A. *Res. Chem. Intermed.* **2008**, *34*, 127−136. (b) Gerdes, R.; Lapok, L.; Tsaryova, O.; Woehrle, D.; Gorun, S. M. *Dalton. Trans.* **2009**, *7*, 1098−1100. (c) Nazeeruddin, Md. K.; Humphry-Baker, R.; Grätzel, M.; Murrer, B. *Chem. Commun.* **1998**, *6*, 719−720. (d) Piechocki, C.; Simon, J.; Skoulios, A.; Guillon, D.; Weber, P. *J. Am. Chem. Soc.* **1982**, *104*, 5245−5247. (e) Winter, G.; Heckmann, H.; Haisch, P.; Eberhardt, W.; Hanack, M.; Lueer, L.; Egelhaaf, H.; Oelkrug, D. *J. Am. Chem. Soc.* **1998**, *120*, 11663−11673. (f) Cook, M. J.; Dunn, A. J.; Howe, S. D.; Thomson, A. J.; Harrison, K. J. *J. Chem. Soc., Perkin Trans. 1* **1988**, 2453−2458. (g) Hanack, M.; Gul, A.; Hirsch, A.; Mandal, B. K.; Subramanian, L. R.; Witke, E. *Mol. Cryst. Liq. Cryst.* **1990**, *187*, 365−382.

(7) (a) Cong, F.; Ning, B.; Du, X.; Ma, C.; Yu, H.; Chen, B. *Dyes Pigm.* **2005**, *66*, 149−154. (b) Duan, W.; Wang, Z.; Cook, M. J. *J. Porphyrins Phthalocyanines* **2009**, *13*, 1255−1261. (c) Tau, P.; Nyokong, T. *J. Electroanal. Chem.* **2007**, *611*, 10−18.

(8) Yuksel, F.; Tuncel, S.; Ahsen, V. *J. Porphyrins Phthalocyanines* **2008**, *12*, 123−130.

(9) Venkatramaiah, N.; Rocha, D. M. G. C.; Srikanth, P.; Almeida Paz, F. A.; Tome, J. P. C. *J. Mater. Chem. C* **2015**, *3*, 1056−1067.

(10) Gumus, G.; Ahsen, V. *J. Porphyrins Phthalocyanines* **2002**, *6*, 489−493.

(11) Chen, Y.; Cao, W.; Wang, K.; Jiang, J. *Inorg. Chem.* **2015**, *54*, 9962−9967.

(12) (a) Claessens, C. G.; Gonzalez-Rodriguez, D.; Torres, T. *Chem. Rev.* **2002**, *102*, 835−853. (b) de la Torre, G.; Vazquez, P.; Agullo-Lopez, F.; Torres, T. *Chem. Rev.* **2004**, *104*, 3723−3750. (c) Claessens, C. G.; Gonzalez-Rodriguez, D.; Rodriguez-Morgade, M. S.; Medina, A.; Torres, T. *Chem. Rev.* **2014**, *114*, 2192−2277. (d) Swain, D.; Singh, V. K.; Krishna, N. V.; Giribabu, L.; Rao, S. V. *J. Porphyrins Phthalocyanines* **2014**, *18*, 305−315. (e) Qi, D.; Jiang, J. *ChemPhysChem* **2015**, *16*, 1889−1897.

(13) (a) D'Souza, S.; Antunes, E.; Litwinski, C.; Nyokong, T. *J. Photochem. Photobiol., A* **2011**, *220*, 11−19. (b) Han, M.; Zhang, X.; Zhang, X.; Liao, C.; Zhu, B.; Li, Q. *Polyhedron* **2015**, *85*, 864−873. (c) Patrick, D. A.; Bakunov, S. A.; Bakunova, S. M.; Kumar, E. V. K. S.; Lombardy, R. J.; Jones, S. K.; Bridges, A. S.; Zhirnov, O.; Hall, J. E.; Wenzler, T.; Brun, R.; Tidwell, R. R. *J. Med. Chem.* **2007**, *50*, 2468−2485.

(14) Kobayashi, N.; Nakajima, S.; Ogata, H.; Fukuda, T. *Chem. - Eur. J.* **2004**, *10*, 6294−6312.

DOI: 10.1021/acs.inorgchem.6b00100
Inorg. Chem. XXXX, XXX, XXX−XXX

(15) Kadish, K. M., Smith, K. M., Guilard, R., Eds. *Handbook of Porphyrin Science*; World Scientific Publishing: Singapore, 2010; Vol. 9.
(16) Jiang, J.; Bao, M.; Rintoul, L.; Arnold, D. P. *Coord. Chem. Rev.* **2006**, *250*, 424−448.
(17) (a) Zhang, R. *Scientific Computing with Python*; Tsinghua University Press: Beijing, China, 2012; Chapter 15, pp 505−536. (b) The testing sample of M{Pc[N(C_4H_9)$_2$]$_4$} (M = 2H, Mg, Cu, Zn) is the mixture of four regioisomers including M{Pc[N(C_4H_9)$_2$]$_4$-C_4}, M{Pc[N(C_4H_9)$_2$]$_4$-C_1}, M{Pc[N(C_4H_9)$_2$]$_4$-C_s}, and M{Pc[N(C_4H_9)$_2$]$_4$-C_{2v}]}. For example, in Figure 3, the CV curve for the first oxidation process of **4** can be divided into four peaks using LCI analysis because of the different first oxidation potentials of these four molecules. In this case, the traditional analysis method, Oxd_1 = [potential B + potential E]/2 = [peak II (upper curve) + peak IV (lower curve)]/2, is physically meaningless because of the overlapped cyclic voltammograms independently expressed by these four regioisomers..
(18) (a) Becke, A. *J. Chem. Phys.* **1993**, *98*, 5648−5652. (b) Lee, C.; Yang, W.; Parr, R. *Phys. Rev. B: Condens. Matter Mater. Phys.* **1988**, *37*, 785−789. (c) Miehlich, B.; Savin, A.; Stoll, H.; Preuss, H. *Chem. Phys. Lett.* **1989**, *157*, 200−206. (d) Boese, A.; Handy, N. *J. Chem. Phys.* **2002**, *116*, 9559−9569. (e) In the theoretical simulation of absorption spectra, the validity of the functional *τ*HCTHhyb is described in the SI..
(19) (a) Hay, P. J.; Wadt, W. *J. Chem. Phys.* **1985**, *82*, 270−283. (b) Wadt, W. R.; Hay, P. J. *J. Chem. Phys.* **1985**, *82*, 284−298. (c) Hay, P. J.; Wadt, W. *J. Chem. Phys.* **1985**, *82*, 299−310.
(20) (a) Ren, Q.; Chen, Z.; Ren, J.; Wei, H.; Feng, W.; Zhang, L. *J. Phys. Chem. A* **2002**, *106*, 6161−6166. (b) Tong, Y.-P.; Lin, Y.-W. *J. Mol. Struct.: THEOCHEM* **2010**, *952*, 61−66. (c) Tong, Y.-P.; Lin, Y.-W. *Spectrochim. Acta, Part A* **2011**, *78*, 809−817. (d) Qi, D.; Zhang, L.; Wan, L.; Zhao, L.; Jiang, J. *J. Phys. Chem. A* **2012**, *116*, 6785−6791.
(21) Mayer, I. *Chem. Phys. Lett.* **1983**, *97*, 270−274.
(22) (a) Qi, D.; Zhang, L.; Zhang, Y.; Bian, Y.; Jiang, J. *J. Phys. Chem. A* **2010**, *114*, 13411−13417. (b) Qi, D.; Jiang, J. *J. Phys. Chem. A* **2011**, *115*, 13811−13820.
(23) Sheik-Bahae, M.; Said, A. A.; Van Stryland, E. W. *Opt. Lett.* **1989**, *14*, 955−957.
(24) Sheik-Bahae, M.; Said, A. A.; Wei, T. H.; Hagan, D. J.; Van Stryland, E. W. *IEEE J. Quantum Electron.* **1990**, *26*, 760−769.

DOI: 10.1021/acs.inorgchem.6b00100
Inorg. Chem. XXXX, XXX, XXX−XXX